Growth Mechanism of Long Aligned Multiwall Carbon Nanotube Arrays by Water-Assisted Chemical Vapor Deposition

YeoHeung Yun,[†] Vesselin Shanov,[‡] Yi Tu,[§] Srinivas Subramaniam,[‡] and Mark J. Schulz*,[†]

Department of Mechanical Engineering, Smart Materials Nanotechnology Laboratory, University of Cincinnati, Cincinnati, Ohio 45219, Department of Chemical and Materials Engineering, University of Cincinnati, Cincinnati, Ohio 45219, and First Nano a Division of CVD Equipment Corporation, 1860 Smithtown Avenue, Ronkonkoma, New York 11779

Received: December 8, 2005; In Final Form: August 12, 2006

Highly aligned arrays of multiwalled carbon nanotube (MWCNT) on layered Si substrates have been synthesized by chemical vapor deposition (CVD). The effect of the substrate design and the process parameters on the growth mechanism were studied. Adding water vapor to the reaction gas mixture of hydrogen and ethylene enhanced the growth which led to synthesis of longer CNT arrays with high density. Environmental scanning electron miscroscopy (ESEM), energy-dispersive spectroscopy (EDS), and atomic force microscopy (AFM) were used to analyze the CNT morphology and composition. Quadrupole mass spectroscopy (QMS) provided in-situ information on the gas spices within the reaction zone. On the basis of results, we verified the top growth mechanism and evaluated the reason of decline and stoppage of the CNT growth after extended period of deposition. Multilayered Si substrates with a top film of Al_2O_3, having appropriate roughness, provide favorable conditions to form catalyst islands with uniform distribution and size. Using water-assisted CVD process and optimized substrate design, our group succeeded to grow vertically aligned, patterned MWCNT up to 4-mm long. The arrays were of high purity and weak adhesion which allowed to be peeled off easily from the substrate.

Introduction

Synthesis, processing, and device fabrication techniques for carbon nanotube (CNT) growth have recently been improved with the help of intensive research and material characterization. However, there still are many challenges to fabricating tailored practical devices because of uncontrollable properties of the CNT growth. One solution is to develop vertically aligned arrays of CNT which have well-defined properties with uniform length and diameter. Our group has successfully reported biosensor applications on the basis of long CNT array.[1] Thermally driven chemical vapor deposition (CVD) using catalytically patterned surfaces offers unique advantages to grow high-density CNT. The thermally driven CVD method uses hydrocarbon precursor molecules (CH_4, C_2H_2, C_2H_4, etc.) for the carbon source, and Fe, Ni, and Co are used as catalysts to grow high-density arrays on Si substrates. The growth mechanism is still controversial and is essentially divided into base growth and tip growth models. Growth mechanism is studied[2] on the basis of the strength of the interaction between the nanoparticle and the support. Still, growth kinetics of CNT is a complicated phenomenon on the basis of condensed matter self-organization, which has been studied on the basis of in-situ observation[3] and molecular dynamics.[4] The growth mechanism of CNT arrays on patterned substrates is explained on the basis of experimental results.[5]

Multiwall carbon nanotube (MWCNT) arrays using the floating catalyst, ferrocene, $Fe(C_2H_5)_2$ is synthesized.[6] This precursor for in-situ Fe formation enhances the effectiveness of the predeposited catalyst film resulting in a higher CNT growth rate. The efficient CVD synthesis of SWCNT where the activity of the catalyst is enhanced by water during the synthesis is demonstrated.[7] Their group grew 2.5-mm-long SWCNT forests using water-stimulus which oxidizes amorphous carbon without damaging the nanotubes. The diffusion kinetics of CNT formation with water-assisted catalyst should be studied further. The current paper presents experimental results which provide clues to understanding the water-assisted growth mechanism. Especially, this paper focuses on MWCNT array growth for potential immunosensor development.[1] Quadrupole mass spectroscopy (QMS) is used to analyze the behavior of water-assisted MWCNT growth. Growth parameters including flow rates, water vapor delivery, temperature, time, catalyst type, and film thickness on the Si wafer are carefully considered in this paper. Environmental scanning electron microscopy (ESEM), high-resolution transmission electron microscopy (HRTEM), and atomic force microscopy (AFM) results before and after MWCNT growth provide understanding of the growth kinetics and relationships between the Fe catalyst, Al_2O_3, and SiO_2 on the Si wafer and the MWCNT array morphology including nanotube diameter and length.

Experimental Procedure

P-type Si wafers ⟨100⟩ with 4-in. diameter and a typical resistivity of 1−20 Ohm-cm are used, and some samples have a 500-nm SiO_2 layer on the top. Then, an e-beam evaporator is used to deposit Al thin film about 10-nm thick, and the Al is

* Author to whom correspondence should be addressed. Tel: (513) 556-4132; fax: (513) 556-3390; e-mail: Mark.J.Schulz@uc.edu.
[†] Department of Mechanical Engineering, University of Cincinnati.
[‡] Department of Chemical and Materials Engineering, University of Cincinnati.
[§] First Nano a Division of CVD Equipment Corporation.

10.1021/jp057171g CCC: $33.50
Published on Web 11/07/2006

oxidized to convert to Al_2O_3. Finally, catalytic iron films of controlled thickness 1−2 nm are deposited on the surface of Si, SiO_2, and Al_2O_3 surfaces. The evaporation is carried out at a pressure of about 5×10^{-7} Torr, and the system is equipped with a film thickness monitor. The final substrate is cut in 5 × 5 mm size wafers. Various masks are used to make two-dimensional patterns on the substrate.

Nanotube array synthesis by thermal CVD is carried out in a horizontal 2-in. tube furnace, the EasyTube (ET1000, First-Nano), which consists of four mass flow controllers and a vapor delivery system. Argon is used as the carrier gas to carry the water vapor to the reaction chamber. Argon is also used to purge the reactor for 20 min while the CVD furnace is heated to 750 °C. Gas flow is then switched to ethylene, water, and hydrogen for the desired time of the deposition phase. After synthesis, the nanotube array is cooled to ambient temperature, which completes the last process step. During the cooling process, ethylene, water, and hydrogen flow is stopped and the system is purged with argon to prevent backflow of air from the exhaust line.

The synthesized MWCNT arrays are characterized by ESEM coupled with energy-dispersive spectroscopy (EDS). Even though EDS does not provide a highly accurate concentration, EDS rapidly (∼5 s) provides information about the chemical characteristics of a sample, and EDS is coupled with the ESEM. To investigate the gas-phase environment during the nanotube growth, the EasyTube system was modified by incorporating a quadrupole mass spectrometer, VISION 1000 P-M (300 amu), made by MKS Instruments. This instrument samples from the reactor during the deposition and provides quick feedback information about the species in the reaction zone. The QMS approach helps to optimize the process variables in terms of quality of the MWCNT. Sampling of the gas phase is done through a heated capillary inserted inside of the reactor. The capillary is connected to the QMS sensor via a pressure-reducing system, allowing measurement at close to atmospheric pressure in the CVD reactor. The synthesized MWCNT arrays are examined by HRTEM. First CNT arrays are harvested from the substrate and are dispersed in dimethylformamide (DMF) using tip ultrasonication (Fisher) without any purification steps. HRTEM samples were prepared by placing a small droplet of the dispersion onto grids (Leci carbon support grid and Leci carbon TM grid, TED PELLA.Com) and drying in air. A JEOL JEM-2010 F TEM operated at 200 kV is used for imaging.

Experimental Results

Figure 1a−d shows ESEM results at different growth times with the assistantance of water while fixing the other growth conditions: 500 standard cubic centimeters per minute (SCCM) of H_2 flow, 700 SCCM of C_2H_4 flow, and a 750 °C growth temperature. The $Fe/Al_2O_3/SiO_2/Si$ substrate is cut into 5-mm squares from one wafer and Fe is patterned on 1-mm squares with 100-μm spacing between the blocks. It is assumed that all growth conditions are the same except the growth time. With the increase of growth time, the length of the CNT arrays increases for up to 3 h. Bower et al. showed that the nanotubes grow quickly in the first 15 min and then the growth rate sharply decreases.

The MWCNT array has high density without many impurities, which is ideal for further application development. Adhesion to the substrate is weak, and the MWCNT array is easily peeled off. In the case of the 15-min growth, the MWCNT array has a perfect edge with a uniform top surface, but alignment of MWCNT arrays becomes worse with the longer MWCNT array. Figure 1c shows one bundle of a MWCNT array block which

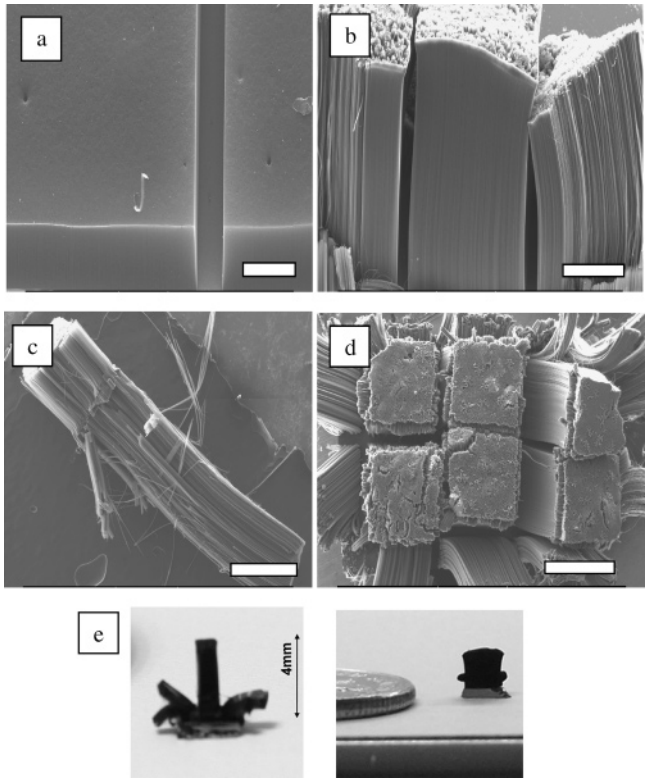

Figure 1. ESEM images of aligned MWCNT patterned arrays showing the effect of growth time: (a) 15 min (scale 200 μm); (b) 1 h (scale 200 μm); (c) 3 h (scale 1 mm); (d) 6 h (scale 1 mm), top view; and (e) picture of 4-mm-tall MWCNT patterned arrays on a Si wafer.

is removed from the array using tweezers without damage. The MWCNT array is easily harvested from the substrate for use in futuristic applications. Our group[8] reported the influence of the intermediate buffer layer, Al_2O_3 (10 nm), in the growth of MWCNT arrays with Fe used as the active catalyst, which is the most effective way to grow long, high-density MWCNT arrays. This paper also confirms the role of intermediate buffer layer which prevents diffusion from the substrate, creates roughness, and creates an environment for catalyst nucleation sites. The density of the nucleation sites (number of sites per square area) potentially can be tailored to produce a dense array or a sparse array. The Fe collapsing from a continuous film to active sites is studied in detail. At the same time, SiO_2 on Si helps to prevent chemical reactions since pure Si can react with various catalysts, and the C in the catalyst might form silicates and C-silicate. Therefore, a chemically inert layer like SiO_2 helps to grow longer MWCNT arrays with high purity. A Mo (∼0.2 nm) layer on the top of iron to increase the yield of nanotubes is another approach,[10,11] but still more careful study is needed to understand the effect of the catalysts. Figure 1e shows a 4-mm-tall MWCNT patterned array on a Si wafer and a coin for size reference.

Figure 2a−c shows ESEM images of high-density MWCNT arrays at high magnification, 20 000×, and the scale bar is 1000 nm. Figure 2d shows the highest magnification of Figure 2c, 100 000×, and the scale bar is 200 nm. With increased growth time, the CNT array is aligned better. Figure 2 also shows the effect of growth time on nanotube thickness. Figure 2a−c shows the nanotube diameter increases from 10 to 50 nm for growth times of 30 min to 6 h. Figure 2a has a much smaller diameter MWCNT, about 10−20 nm. The increasing wall thickness and alignment with longer growth time forms strong bundles which might be ideal for future composite materials applications.

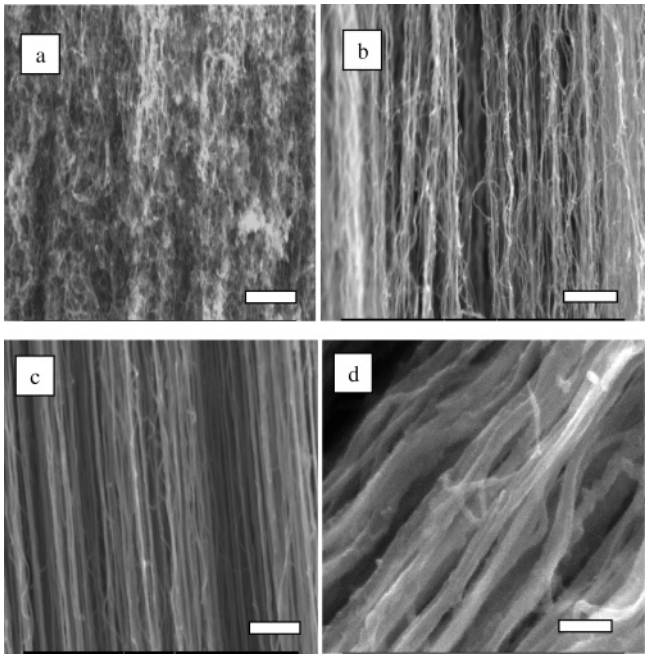

Figure 2. ESEM images of aligned MWCNT patterned arrays showing the effect of growth time: (a) 15 min (scale 1 μm); (b) 3 h (scale 1 μm); (c) 6 h (scale 1 μm), for a−c magnification is 20 000×; and (d) high magnification 100 000× of Figure 2c (scale bar is 200 nm).

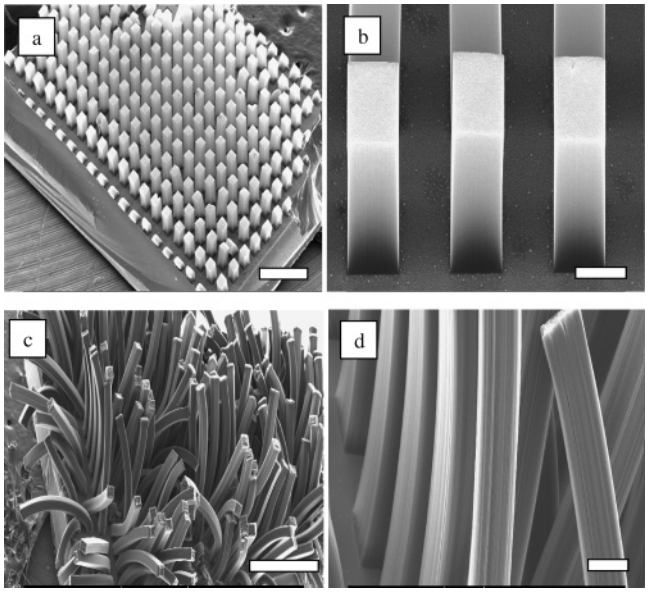

Figure 3. ESEM images of aligned MWCNT patterned arrays showing the effect of alignment with growth time: (a) half hour, top view (scale 1 mm); (b) half hour, side view (scale 100 μm); (c) 3 h, top view (scale 1 mm); and (d) 3 h, side view (scale 100 μm).

Figure 2d shows the highest magnification of Figure 2c, 100 000× with a 200-nm scale bar, for the 3-h growth time experiment resulting in high alignment with 30−40 nm diameter MWCNT. More experiments are planned to explain how the MWCNT can increase diameter using transmission electron microscopy and Raman spectroscopy characterization. Graphitic phase of the carbon nanotubes or possible coating of amorphous carbon on the MWCNT should be studied properly in the future.

Figure 3 shows ESEM images of aligned MWCNT patterned arrays showing the effect of alignment with growth time. Fe is patterned in 100 μm × 100 μm blocks with 100-μm spacing between blocks. As shown in Figure 3a, MWCNT patterned arrays are grown straight and parallel up to 0.2-mm long. Longer

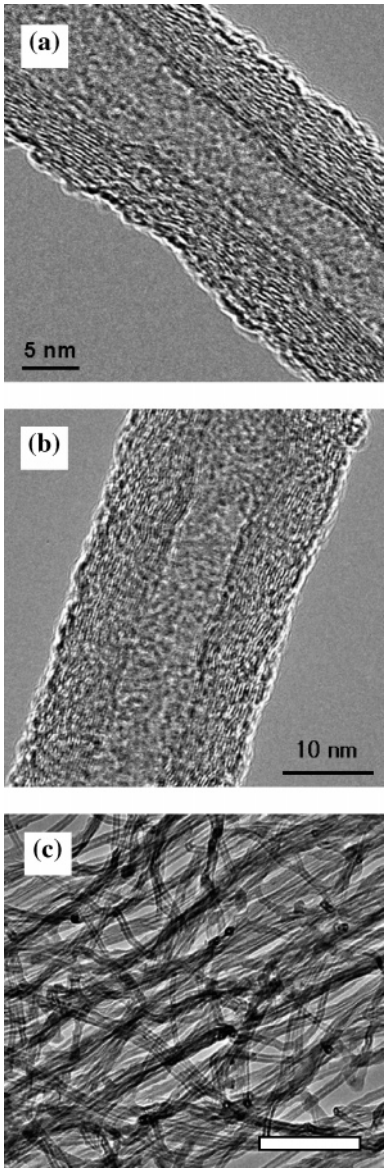

Figure 4. TEM images using a JEOL JEM-2010, 200 kV showing the MWCNT structure with 15−20 nm diameter at (a, b) high resolution and (c) lower resolution (scale 200 nm).

arrays in Figure 3c did not grow straight and parallel. The nonuniformity of the catalyst on the top might be the reason for MWCNT array bends. Also, closer spacing of the towers will be investigated to prevent bending. Even though individual MWCNT towers are bent, every MWCNT tower has high density and purity (Figure 3b, d).

Figure 4 shows HRTEM images of the center plane of the nanotubes with high magnification illustrating the high quality of nanotubes without metal catalyst particles or amorphous carbon. Figure 4a is a high-resolution TEM image showing that the MWCNTs have 15−20 nm outer diameters and 5−8 nm inner diameters with 15 walls on average. The white dots are individual carbon atoms, and the lines of dots are the walls of the nanotube. As shown in Figure 4b, diameters of nanotubes appear uniform without impurities. Figure 4c shows the uniformity of the MWCNT at lower magnification.

Discussion and Characterization

In the MWCNT growth time at 750 °C, the Fe catalyst on the Al_2O_3 starts to form a liquid nanoparticle of metal which is

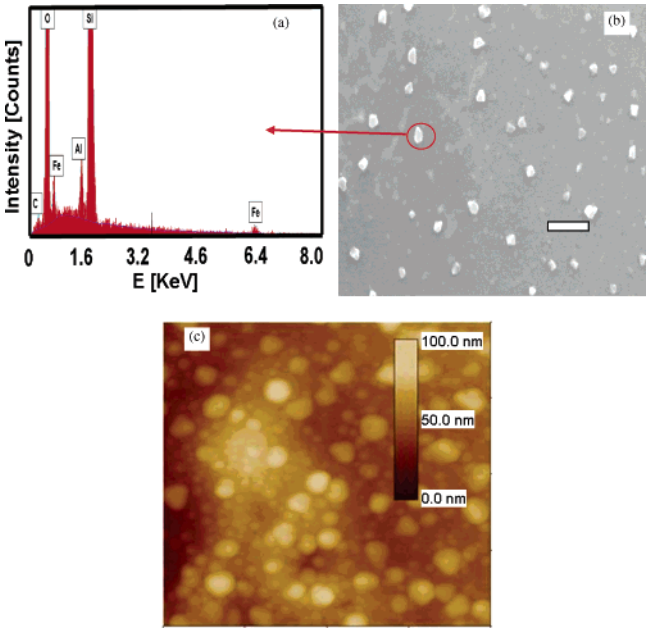

Figure 5. EDS (a), ESEM (scale 500 nm) (b), and AFM (c) images of the iron catalyst particle distribution on top of a SiO_2/Al_2O_3 layered silicon substrate. The substrate is annealed in air for 5 h at 400 °C and then is thermally treated in the nanofurnace for 10 min with the normal growth recipe but without ethylene flow (200 H_2, 100 Ar with H_2O, $T = 750$ °C).

supersaturated with carbon provided by the hydrocarbon precursor molecules, C_2H_4. The most critical factor is the size of the nanoparticle island which is determined by the substrate roughness and reaction parameters, such as the gas flow rate and the temperature gradient. In our case, the intermediate buffer layer Al_2O_3 provides high roughness which makes the nanoparticle island smaller. The diameter of the MWCNT is proportional to the size of the catalyst island.[11]

Figure 5 illustrates EDS, ESEM, and AFM images to study the iron catalyst particle distribution on top of a SiO_2/Al_2O_3 layered silicon substrate. The substrate is annealed in air for 5 h at 400 °C and then is thermally treated in the nanofurnace for 10 min with the normal growth recipe but without ethylene flow (200 H_2, 100 Ar with H_2O, $T = 750$ °C). The catalyst particle diameters range from 15 to 50 nm, and the catalyst is uniformly distributed over the surface of the substrate. The chemical composition of catalyst particle is mostly Fe and Al_2O_3. The catalyst particle diameter is critical to promote oriented growth of the array and to control the diameter of the nanotubes. Since EDS penetrates up to 10 μm of Fe, possibly Al comes from the Al_2O_3 layer and oxygen comes from the chamber. Two different peaks of Fe come from two different orbits of Fe atom. Growth mechanism is divided on the basis of the adhesion to the substrate surface.[11] In our case, the top growth model is reasonable for high-density aligned MWCNT forest since carbon species may be unable to penetrate to the forest bottom. Also, Fe adhesion to substrate is not strong to enough to hold the Fe on the bottom since the Fe islands are small and the Al_2O_3 is a thin intermediate buffer layer. Figure 6 shows the EDS results of the top and bottom portion of an MWCNT array. The MWCNT array sample was positioned vertically in the ESEM which allowed a large portion of the array to be investigated by EDS. When studying the bottom part of the MWCNT array, the only detected elements were C from the nanotubes and Si from the substrate. Surprisingly, no Fe catalyst was found. However, the EDS analysis of the top part of the MWCNT array shows the presence of C, Si, O, and Fe. The oxygen comes from the exposure of the nanotubes to the air prior to the microscopy.

Another way to detect iron is using backscattered electrons (BSE) which provide good contrast. Figure 7 shows ESEM (a) and backscattered electron (b) images of iron nanoparticles on top of the MWCNT array grown in 1 h. We can see the iron catalyst nanoparticles on the top of a nanotube array (bright particle images). These results suggest that in our experiments the top growth mechanism of MWCNT growth occurs. We assume that the catalyst is transported to the top by the growing nanotubes because of the relatively weak adhesion between the aluminum oxide buffer layer and the catalyst film on top of it. Another interesting result is that no Fe could be detected even on the top of MWCNT array when running the furnace more than 3 h. Probably, the Fe catalyst is depleted when the furnace is run for a long time. Instead, amorphous carbon or graphite starts to form on the top of the array. The bottom growth might occur because the metallic nature of the buffer layer increases adhesion of the iron catalyst which constrains the catalyst from lifting off the buffer layer.[13]

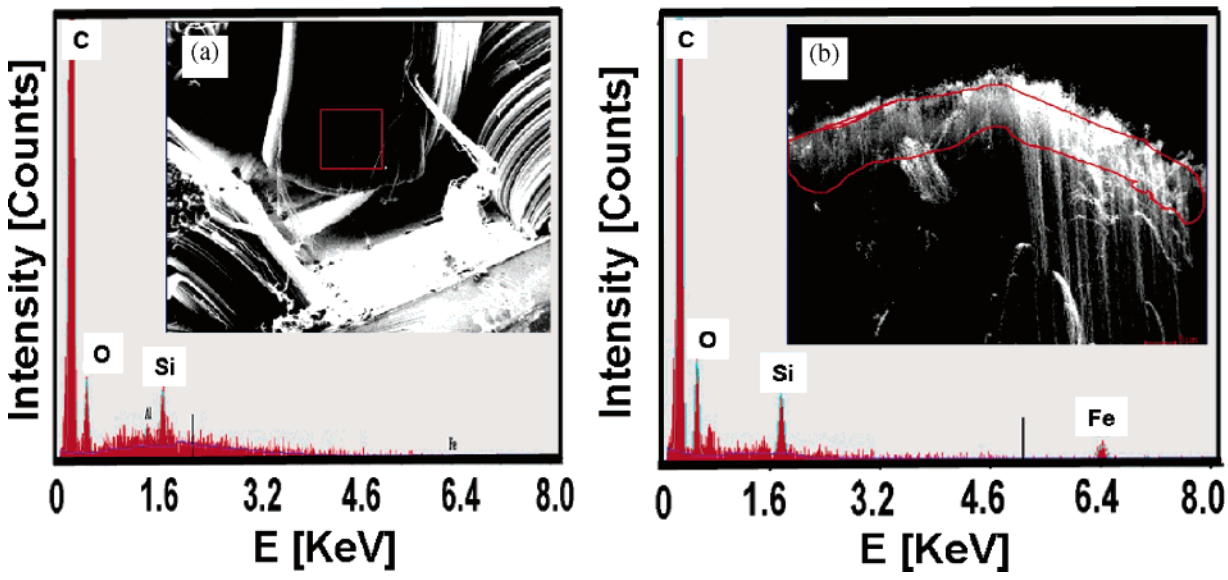

Figure 6. EDS results on the bottom (a) and top (b) parts of the CNT forest array, 1-mm length, 1-h growth, and 100 SCCM water assistance.

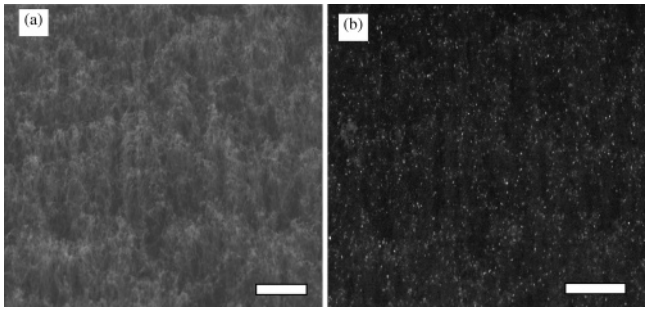

Figure 7. ESEM (scale 2 μm) (a) and backscattered electron (scale 2 μm) (b) images of iron nanoparticles on the top of the carbon nanotube array grown in 1 h.

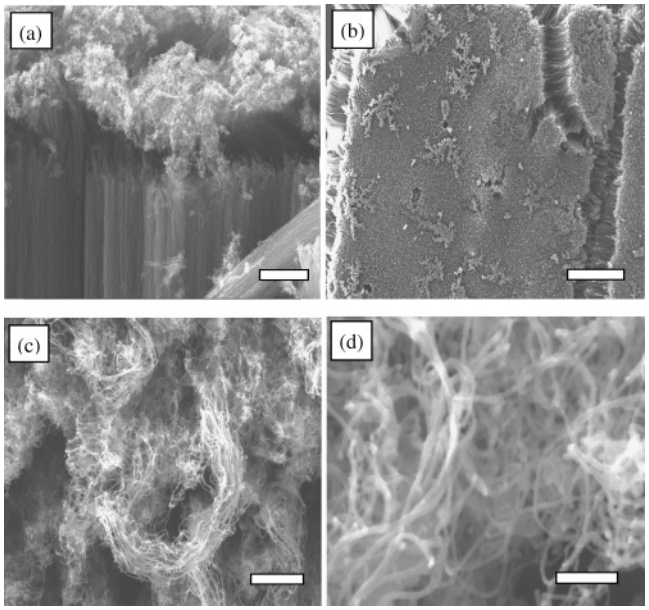

Figure 8. ESEM images of nanotube array illustrating the change in vertical array growth to random growth of bundles on the top of the array: (a) side view of top of array (scale 100 μm) and (b−d) top view from low to high resolution (b scale 200 μm, c scale 2 μm, and d scale 500 μm).

We have a hypothesis to explain why the growth stops. Our hypothesis is that during the growth the catalyst is losing its activity which results in the growth stopping or the growth direction becoming random. The random growth is illustrated in Figure 8 which shows lateral wandering growth of an aligned bundle of carbon nanotubes on top of the array. We postulate two reasons for the growth stopping or changing direction.

The first possible reason for the nanotube growth changing is that amorphous carbon builds up on top of the catalyst active sites and the catalyst becomes partly covered with the dense layer of amorphous carbon which passivates the catalyst. Some of the nanotubes have active catalyst and continue to grow vertically while the growth of nanotubes that have the catalyst depleted slows or stops. The nanotubes that continue growing are not well supported and the partial array growth turns into random lateral growth of bundles of aligned nanotubes. This growth progress is illustrated in Figure 8. The change in the orientation and the diameter of the nanotubes grown on top of the array are shown in Figure 8. The different size and partially blocked catalyst islands on top of the array affect the growth rate and direction. Also, the flow conditions in the reactor can affect the carbon supply and the subsequent growth rate. The overall effect is that certain areas of the array stop growing and other areas maintain the initial high growth rate. In this case, the support provided by the adjacent nanotubes is lost which

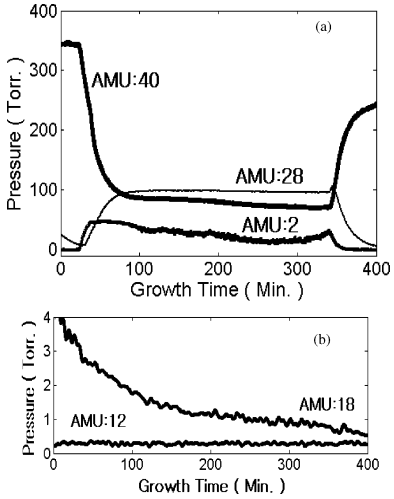

Figure 9. QMS response for variation in partial pressure with time for monitored gaseous species (a) Ar^+, H_2^+, and $C_2H_4^+$ and (b) O_2^+ and C^+.

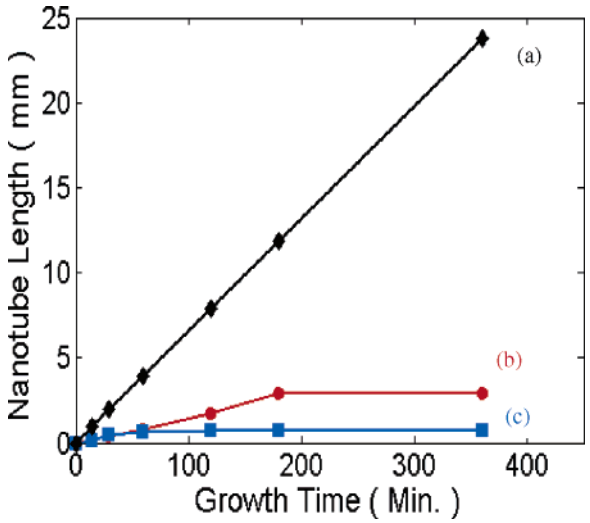

Figure 10. Theoretical prediction (a) and experimental results (b) and (c) of the nanotube length vs growth time. CVD with water-assistance (b) and CVD without water-assistance (c), $Al_2O_3/SiO_2/Si$ substrate is used.

causes bending and winding of the tubes. In addition to the amorphous carbon, other hydrocarbon-based byproducts may be formed in the presence of water which may block the catalyst function by covering the catalyst. To maintain the growth rate, the blocking film must be constantly removed by oxidizing it.

The second possible reason for the nanotube growth stopping is that the catalyst may be depleted by water oxidation, by high-temperature erosion, or by forming stable iron carbides. It is possible that powdered solid particles can be formed on top of the array which may additionally promote nonoriented growth. These particles may be based on iron carbides, Fe_2O_3, Al_2O_3, or related compounds. They may also promote nonoriented growth on top of the array.

In-situ QMS is a powerful technique for monitoring the species in the CVD reactor which helps to understand the nanotube growth. A dynamic mode of data acquisition is employed to track the concentration of the major species with time. This mode easily reveals the changes in the partial pressure of the species when changing the concentration of the reactive gases (hydrogen, water, or ethylene). Figure 9a and b shows a typical QMS response for the variation in partial pressure with time for the monitored gaseous species, Ar^+, H_2^+, $C_2H_4^+$, H_2O^+, and

C^+ during the typical 3-h growth conditions, 200 SCCM ethylene, 100 SCCM bubbler, and 200 hydrogen. Major species (Ar^+, H_2^+, and $C_2H_4^+$) and flow rates of gases were constant after 20 min. However, the carbon partial pressure is very small at roughly 0.4 Torr which is shown in the inset in Figure 9. The QMS monitoring of MWCNT array growth is a new area of investigation, and further investigation is needed to tie QMS results to nanotube growth. The maximum growth rate is 1.2 μm/s in theory and is 0.8 μm/s on the basis of in-situ measurement.[11,12] As shown in our experiments, the water vapor supply enhanced catalyst life and maintained a constant growth rate up to 3 h (Figure 10b). Ideas to increase the nanotube length after 3 h are to (i) increase the water flow, (ii) decrease the precursor flow, or (iii) replenish the catalyst. Figure 10a shows the theoretical prediction of nanotube growth on the basis of the equation which means theoretically CNT can grow 3 cm in 6 h. Further study to find the optimal reaction parameters is needed in the future.

Conclusions

Several conclusions follow from the work in this paper. Water vapor delivery substantially enhanced the catalyst life and allowed synthesis of multiwall carbon nanotube arrays up to 4 mm in height for a 3-h growth time. The nanotube top growth mechanism for these experiments was predicted on the basis of atomic force microscopy and environmental scanning electron microscopy results. The characterization study showed catalyst island formation before nanotube array growth and nanotube growth on the top of the array. On the basis of the characterization results, the reason for nanotube growth stopping was hypothesized and approaches for continuing the growth were suggested.

Acknowledgment. This work was supported in part by the University of Cincinnati Institute for Nanoscale Science and Technology. This support is gratefully acknowledged.

References and Notes

(1) Yun, Y. H.; Shanov, V.; Schulz, M. J.; Dong, Z. Y.; Jaziehc, A.; Heineman, W. R.; Halsall, B. H.; Wong, D. K. Y.; Bange, A.; Tu, Y.; Subramaniamb, S. *Sens. Actuators, B* **2006**, accepted.

(2) Vinciguerra, V.; Buonocore, F.; Panzera, G.; Occhipinti, L. *Nanotechnology* **2003**, *14*, 655.

(3) Louchev, O. A. *J. Cryst. Growth* **2002**, *65*, 237.

(4) Louchev, O. A.; Sato, Y.; Kanda, H. *Appl. Phys. Lett.* **2002**, *80* (15), 2752.

(5) Vajtai, R.; Wei, B. Q.; Ajayan, P. M. *Philos. Trans. R. Soc. London, Ser. A* **2004**, *362*, 2143.

(6) Eres, E.; Puretzky, A. A.; Geohegan, D. B.; Cui, H. *Appl. Phys. Lett.* **2004**, *84* (10), 1759.

(7) Hata, K.; Futaba, D. N.; Mizuno, K.; Namai, T.; Yumura, M.; Ijima, S. *Science* **2004**, *306*, 1362.

(8) Yun, Y. H.; Shanov, V.; Schulz, J. M.; Tu, Y.; Yarmolenko, S.; Neralla, S. *Mater. Chem. Phys*. **2006**, submitted for publication.

(9) Lacerda, R. G.; Teo, K. B. K.; Teh, A. S.; Yang, M. H.; Dalal, S. H.; Jefferson, D. A.; Durrell, J. H.; Rupesinghe, N. L.; Roy, D.; Amaratunga, G. A. J.; Milne, W. I. *J. Appl. Phys.* **2004**, *96* (8), 4456.

(10) Delzeit, L.; Nguyen C. V.; Chen, B.; Stevens, R.; Cassell, A.; Han, J.; Meyyappan, M. *J. Phys. Chem. B* **2002**, *106*, 5629.

(11) Tibbets, G. G. *J. Cryst. Growth* **1984**, *66*, 632.

(12) Klinke, C.; Bonard, J. M.; Kern, K. *Phys. Rev. B* **2005**, *71*, 035403.

(13) Christen, H. M.; Puretzky, A. A.; Cui, H.; Belay, K.; Fleming, P. H.; Geohegan, D. B.; Lowndes, D. H. *Nano Lett.* **2004**, *4* (10), 1939.

(14) Puretzky, A. A.; Geohegan, D. B.; Jesse, S.; Ivanov, I. N.; Eres G. *Appl. Phys. A* **2005,** *81*, 223.

(15) Bower, C.; Zhou, O.; Zhu, W.; Werder, D. J.; Jin, S. *J. Appl. Phys. Lett.* **2000**, *77* (17), 2767.